

Cubic Transmuted Ailamujia Distribution - Type I: Statistical Properties and Application

Jones Asante Manu^{1, *}, Samuel Darkwah²

¹Business Studies Department, Lancaster University Ghana, Accra, Ghana

²Mathematics Department, Methodist University Ghana, Accra, Ghana

Email address:

j.asantemanu@lancaster.edu.gh (Jones Asante Manu), sdarkwah@mucg.edu.gh (Samuel Darkwah)

*Corresponding author

To cite this article:

Jones Asante Manu, Samuel Darkwah. (2024). Cubic Transmuted Ailamujia Distribution - Type I: Statistical Properties and Application. *International Journal of Statistical Distributions and Applications*, 10(3), 60-77. <https://doi.org/10.11648/j.ijds.20241003.12>

Received: 8 July 2024; **Accepted:** 20 September 2024; **Published:** 31 October 2024

Abstract: This study introduces and evaluates the Cubic Transmuted Ailamujia Distribution (CTAD), a novel distribution developed using CRT-type I as a generator and the Ailamujia distribution as a baseline. We derived several statistical quantities, including density and distribution functions, hazard and survival functions, moments, and order statistics. The performance of the CTAD was compared against several established models using three distinct datasets: exceedances of flood peaks from the Wheaton River (Dataset I), cumulative COVID-19 death counts for Ghana (Dataset II), and daily confirmed COVID-19 cases for Ghana (Dataset III). The CTAD showed competitive performance, often outperforming traditional models such as the QTAD and Ailamujia distributions in Dataset I, and demonstrating strong performance relative to the CTGD, CTFD, and CTWD distributions in Dataset II. In Dataset III, while the CTAD was competitive, it was outperformed by the EWD and GGD in terms of AIC and BIC. Overall, the CTAD proves to be a robust and flexible distribution for modelling complex data patterns, though alternative distributions may offer better fits in specific scenarios. These findings underscore the CTAD's potential as a valuable tool in statistical modelling and suggest opportunities for further research and refinement.

Keywords: Ailamujia Distribution, Cubic Rank Transmutation, Maximum Likelihood Estimation, Order Statistics, Moments, Simulation

1. Introduction

The development of new or modified statistical distributions is crucial in the evolving landscape of data analysis and modelling. Traditional distributions, such as the normal, exponential, or gamma distributions, often work well for standard datasets with well-understood characteristics. However, real-world data frequently exhibit more complex behaviours that cannot be adequately captured by these classical distributions. Phenomena such as skewness, kurtosis, heavy tails, and multimodal patterns are commonly encountered in modern datasets across various fields, including finance, biology, engineering, and social sciences. These complexities necessitate the development of new distributions that are more flexible and can better accommodate the intricacies of real-world data.

One key area where new distributions have become

particularly important is in the modelling of extreme events, such as natural disasters, financial crashes, and pandemics. Classical distributions often fail to capture the heavy-tailed nature of such events, which can lead to underestimation of risk or poor predictive performance. As a result, there has been a growing emphasis on developing generalized distributions (Pearson [14]; Burr [4]; Marshall & Olkin [10]; Eugene et al., [8]; Cordeiro & Castro [7]) that extend existing models to provide greater flexibility. These distributions introduce additional parameters or modifications to the underlying mathematical framework, allowing for better fitting of empirical data.

In this study, the aim was to create a distribution that could handle complex data patterns while offering enhanced adaptability compared to traditional models. By introducing cubic transmutation to the Ailamujia distribution, the new

distribution offers a higher degree of flexibility, making it suitable for datasets with varying skewness and kurtosis, such as those seen in environmental studies, health data, and financial modelling. The ability to adjust the distribution's shape through additional parameters allows for more accurate modelling of real-world phenomena, leading to improved goodness-of-fit, better risk estimation, and more reliable predictions.

1.1. Ailamujia Distribution

Lv et al. [11] developed a single parameter Ailamujia distribution to model a lifetime datasets. The authors examined different statistical properties of the distribution. The Ailamujia distribution has probability distribution function (pdf), $\psi(x)$ given as

$$\psi(x) = \mu^2 x e^{-\mu x}, \quad x \geq 0, \quad \mu \geq 0 \quad (1)$$

Its cumulative distribution function (cdf), $\Psi(x)$ is given by

$$\Psi(x) = 1 - (1 + \mu x) e^{-\mu x}, \quad x \geq 0, \quad \mu \geq 0 \quad (2)$$

For $\lambda_1 \in [0, 1]$ and $\lambda_2 \in [-1, 1]$. $\psi(x)$ and $\Psi(x)$ are the baseline pdf and cdf, respectively.

In this paper, we propose a new three-parameter probability distribution serving as an extension of the Ailamujia distribution based on the CRT. That is, the CRT serves as a generator whilst the Ailamujia distribution serves as the baseline distribution. This distribution's key advantage is its flexibility in modelling more complex data sets. The new distribution will be called the cubic transmuted Ailamujia distribution (CTAD) with three parameters.

The CTAD introduces a significant innovation in statistical modelling through its unique transformation mechanism applied to the Ailamujia distribution. This novel approach combines the robust characteristics of the Ailamujia distribution with cubic transmutation, offering a substantial advancement in modelling complex data patterns. The primary innovation of the CTAD lies in its ability to enhance the flexibility and adaptability of the Ailamujia distribution. Traditional distributions often face limitations when dealing with data exhibiting complex behaviours, such as varying degrees of skewness and kurtosis. By incorporating cubic transmutation, the CTAD introduces additional parameters that allow it to more accurately capture these complexities. This transformation expands the distribution's flexibility, making it suitable for a wider range of empirical data. The cubic transmutation applied in the CTAD provides several advantages over existing distributions. Firstly, it introduces more degrees of freedom, enabling the CTAD to better

In recent years, a lot of attention have been given to this distribution. Several researchers (Aijaz et al. [2], Uzma et al. [18], Rather et al [15], Pan et al, [13]) have studied and provided an array of modifications and extensions to the Ailamujia distribution.

1.2. Cubic Rank Transmutation-Type I

Various methodologies serving as generators have been discussed in the literature. One of such methodology is the rank transmutation maps. Granzotto et al. [9] introduced a second order transmuted distributions called the cubic rank transmutation (CRT) map distribution. CRT distributions are utilized to generate various flexible probability distributions and several researchers (Celik, [5]) have used the CRT to modify various probability distributions. In this study, we refer to the version of the CRT introduced by Granzotto et al. [9] as Type-I, distinguishing it from other versions proposed by researchers such as Al-Kadim & Mohammed [3] and Rahman et al. [16].

The pdf, $g(x)$ and cdf, $G(x)$ of the CRT-Type I are respectively, given as

$$g(x) = \psi(x)[\lambda_1 + 2(\lambda_2 - \lambda_1)\Psi(x) + 3(1 - \lambda_2)\Psi^2(x)] \quad (3)$$

$$G(x) = \lambda_1 \Psi(x) + (\lambda_2 - \lambda_1)\Psi^2(x) + (1 - \lambda_2)\Psi^3(x) \quad (4)$$

accommodate data with skewed or heavy-tailed characteristics. Secondly, this adaptability allows the CTAD to model data with various shapes and distributions more effectively, addressing the limitations of traditional parametric models. In essence, the CTAD represents a notable advancement in distribution modelling by leveraging the strength of cubic transmutation to enhance the Ailamujia distribution. This innovation provides a powerful tool for researchers and statisticians, offering improved fit and flexibility for analyzing diverse data patterns. The CTAD's ability to address complex data structures makes it a valuable addition to the statistical toolkit, paving the way for more nuanced and accurate data analysis.

The paper is organized as follows: Section two discusses the CTAD along with some selected statistical properties. Section three derives the maximum likelihood estimation of the CTAD. In Section four, the CTAD is applied to real datasets to determine the accurateness of maximum likelihood estimators. In Section five, we conclude the paper based on the findings of this paper.

2. Cubic Transmuted Ailamujia Distribution

A three-parameter CTAD using Equations 1, 2 and 4 has its pdf, $g(x)$ given as

$$g(x) = \mu^2 x e^{-\mu x} \left[\lambda_1 + 2(\lambda_2 - \lambda_1) \left[1 - (1 + \mu x)e^{-\mu x} \right] + 3(1 - \lambda_2) \left[1 - (1 + \mu x)e^{-\mu x} \right]^2 \right] \quad (5)$$

where $x > 0$, $\mu > 0$, $\lambda_1 \in [0, 1]$ and $\lambda_2 \in [-1, 1]$

The corresponding cdf, $G(x)$ using Equations 2 and 4, is given as

$$G(x) = \lambda_1 \left[1 - (1 + \mu x)e^{-\mu x} \right] + (\lambda_2 - \lambda_1) \left[1 - (1 + \mu x)e^{-\mu x} \right]^2 + (1 - \lambda_2) \left[1 - (1 + \mu x)e^{-\mu x} \right]^3 \quad (6)$$

where $x > 0$, $\mu > 0$, $\lambda_1 \in [0, 1]$ and $\lambda_2 \in [-1, 1]$.

To illustrate the characteristics of the distribution, the following plots depict the nature and behaviour of its pdf, $g(x)$ and cdf, $G(x)$. These plots illustrate the distribution's shape, central tendency, and spread, offering insights into the variable's behaviour and characteristics.

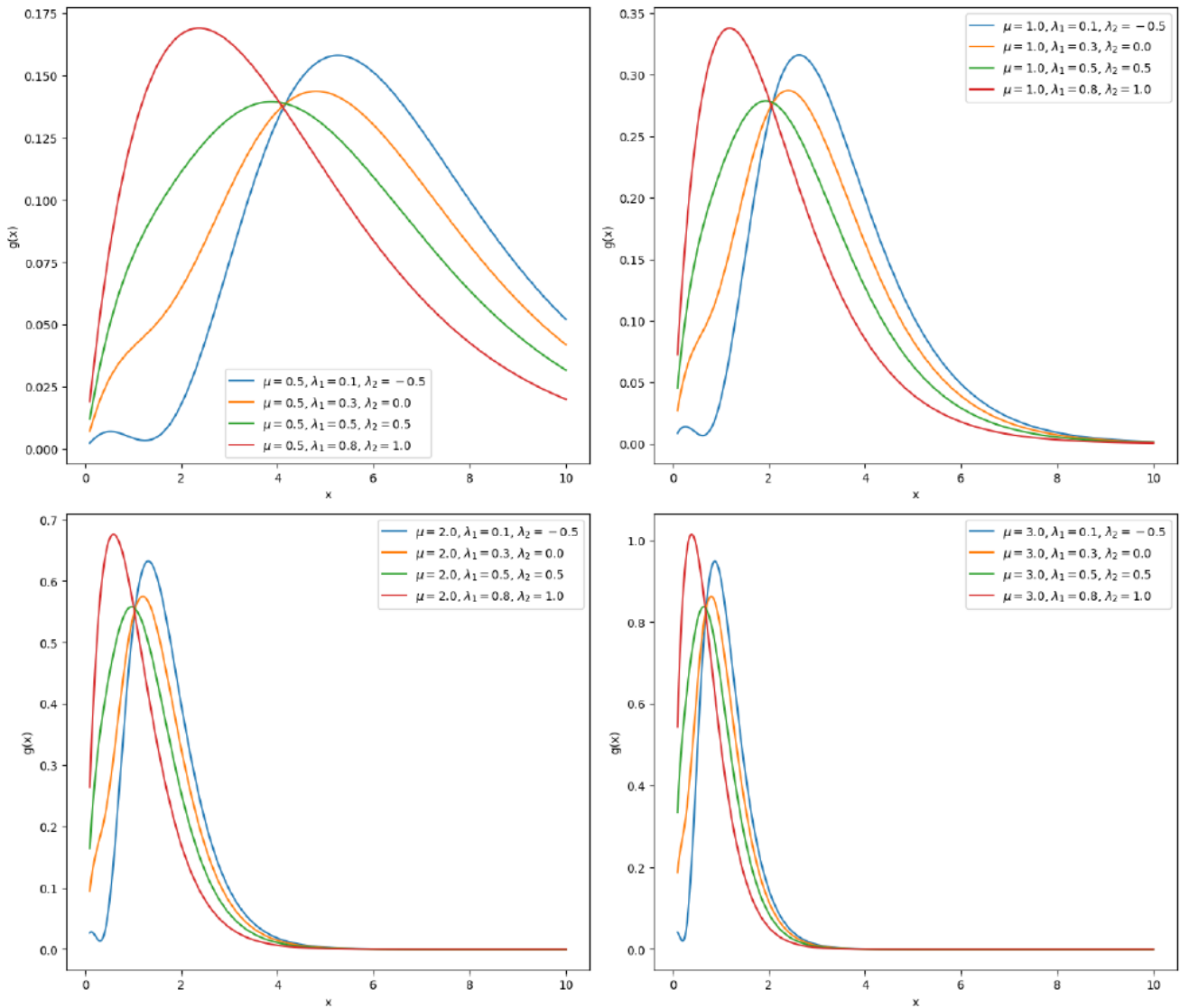


Figure 1. pdf of the CTAD plotted for various parameter values/

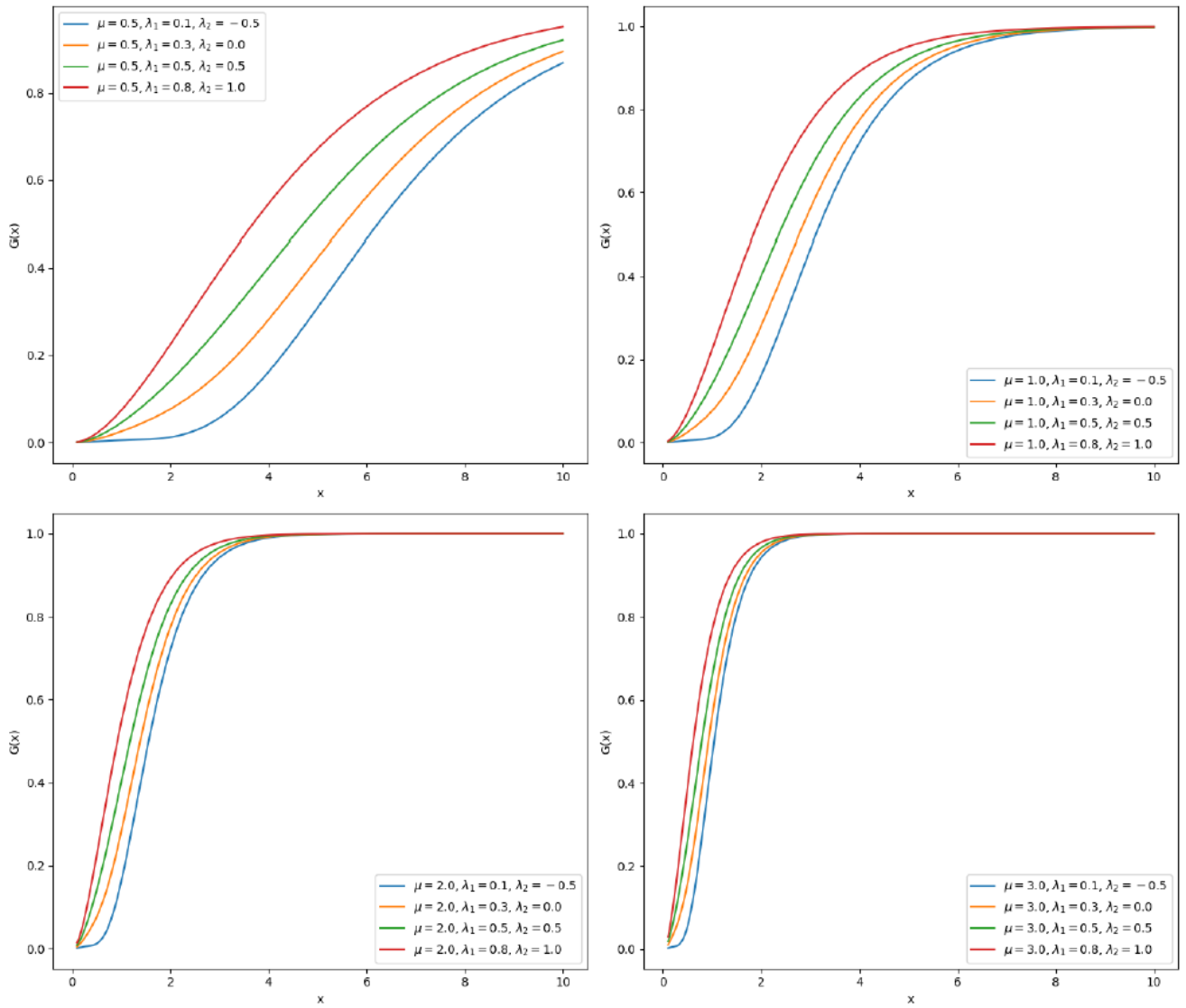


Figure 2. Cdf of the CTAD plotted for various parameter values.

2.1. Survival Function of the CTAD

Let X be a random sample taken from the CTAD. Then its survival function defined as $S(x) = 1 - G(x)$ is given as

$$S(x) = 1 - \left[\lambda_1 \left[1 - (1 + \mu x)e^{-\mu x} \right] + (\lambda_2 - \lambda_1) \left[1 - (1 + \mu x)e^{-\mu x} \right]^2 + (1 - \lambda_2) \left[1 - (1 + \mu x)e^{-\mu x} \right]^3 \right]$$

We plot the $S(x)$ for different parameter values.

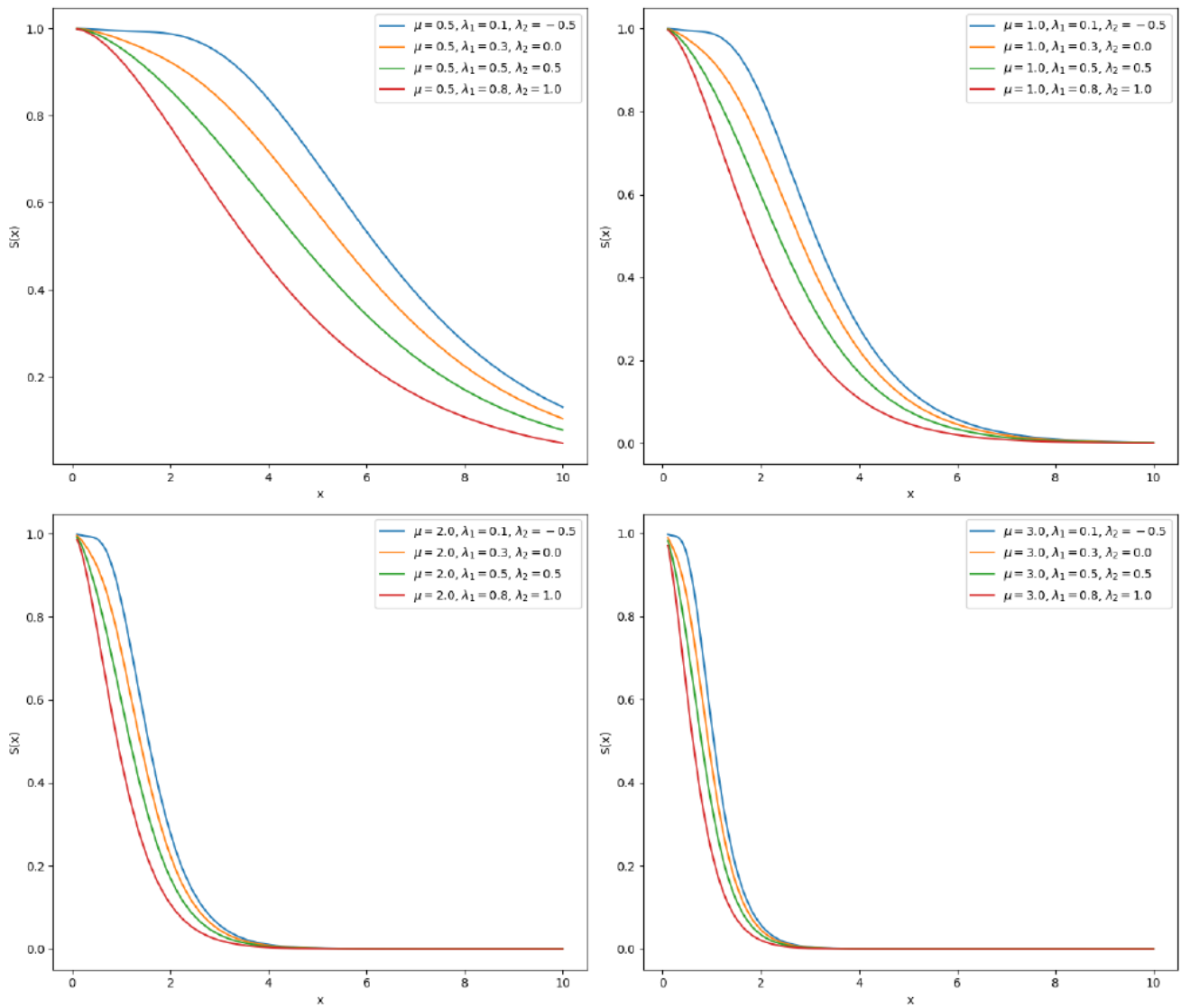


Figure 3. $S(x)$ of the CTAD plotted for different parameter values.

2.2. Hazard Function of the CTAD Distribution

The hazard function is defined as $h(x) = \frac{g(x)}{1 - G(x)} = \frac{g(x)}{S(x)}$. Hence, the $h(x)$ of the CTAD is defined as

$$h(x) = \frac{\mu^2 x e^{-\mu x} \left[\lambda_1 + 2(\lambda_2 - \lambda_1) [1 - (1 + \mu x)e^{-\mu x}] + 3(1 - \lambda_2) [1 - (1 + \mu x)e^{-\mu x}]^2 \right]}{1 - \left[\lambda_1 [1 - (1 + \mu x)e^{-\mu x}] + (\lambda_2 - \lambda_1) [1 - (1 + \mu x)e^{-\mu x}]^2 + (1 - \lambda_2) [1 - (1 + \mu x)e^{-\mu x}]^3 \right]}$$

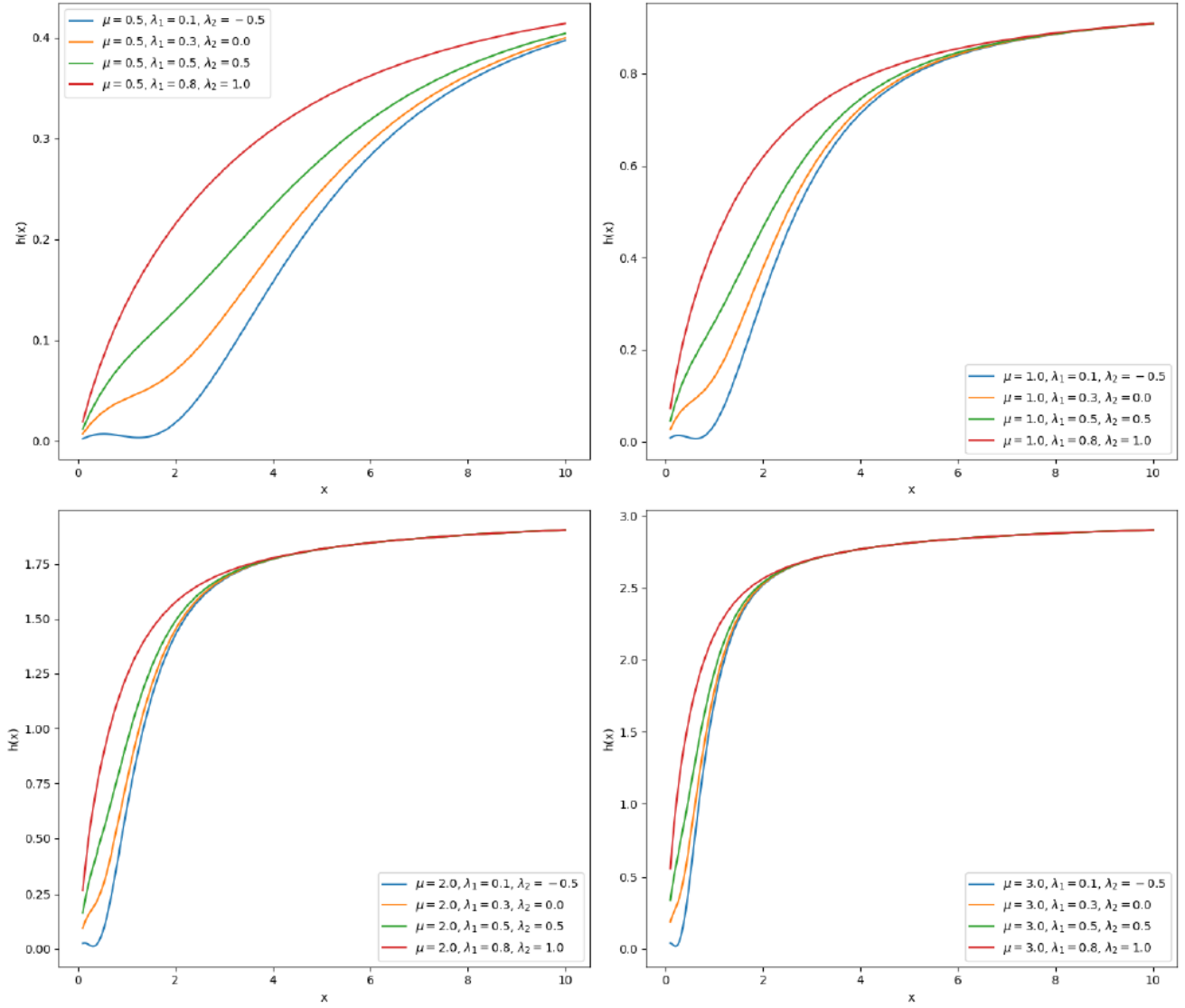


Figure 4. $h(x)$ of the CTAD plotted for different parameter values

2.3. Reverse Hazard Function

The reverse hazard function $h_r(x)$ is defined as: $h_r(x) = \frac{g(x)}{G(x)}$. That is, the $h_r(x)$ of the CTAD is

$$h_r(x) = \frac{\mu^2 x e^{-\mu x} [\lambda_1 + 2(\lambda_2 - \lambda_1) [1 - (1 + \mu x)e^{-\mu x}] + 3(1 - \lambda_2) [1 - (1 + \mu x)e^{-\mu x}]^2]}{\lambda_1 [1 - (1 + \mu x)e^{-\mu x}] + (\lambda_2 - \lambda_1) [1 - (1 + \mu x)e^{-\mu x}]^2 + (1 - \lambda_2) [1 - (1 + \mu x)e^{-\mu x}]^3}$$

2.4. Moments

Moments play a key role in determining various statistical properties. Assuming X is a CTAD random variable with parameters μ , λ_1 , and λ_2 . Then its r^{th} moment is given as

$$\begin{aligned} E[X^r] &= \int_0^\infty x^r g(x) dx \\ &= \int_0^\infty x^r \left[\mu^2 x e^{-\mu x} [\lambda_1 + 2(\lambda_2 - \lambda_1) (1 - (1 + \mu x)e^{-\mu x}) + 3(1 - \lambda_2) (1 - (1 + \mu x)e^{-\mu x})^2] \right] dx \end{aligned}$$

Integrating term by term, we have

$$\begin{aligned}
 E[X^r] &= \int_0^\infty x^r \mu^2 x e^{-\mu x} \lambda_1 dx + \int_0^\infty x^r \mu^2 x e^{-\mu x} 2(\lambda_2 - \lambda_1) (1 - (1 + \mu x)e^{-\mu x}) dx \\
 &\quad + \int_0^\infty x^r \mu^2 x e^{-\mu x} 3(1 - \lambda_2) (1 - (1 + \mu x)e^{-\mu x})^2 dx \\
 &= \mu^2 \lambda_1 \int_0^\infty x^r x e^{-\mu x} dx + \mu^2 2(\lambda_2 - \lambda_1) \int_0^\infty x^r x e^{-\mu x} (1 - (1 + \mu x)e^{-\mu x}) dx \\
 &\quad + \mu^2 3(1 - \lambda_2) \int_0^\infty x^r x e^{-\mu x} (1 - (1 + \mu x)e^{-\mu x})^2 dx
 \end{aligned}$$

This reduces to

$$E(X^r) = -\frac{3^{-r-3} \cdot 2^{-r-2}}{\mu^r} \left\{ \begin{aligned} &[2^{r+2}\Gamma(r+4) + (3 \cdot 2^{r+3} - 2 \cdot 3^{r+3})\Gamma(r+3) \\ &\quad + (3^r(27 \cdot 2^{r+2} - 108) + 9 \cdot 2^{r+2})\Gamma(r+2)]\lambda_2 \\ &+ [3^r(27 \cdot 2^{r+2} - 54)\Gamma(r+2) - 3^{r+3}\Gamma(r+3)]\lambda_1 \\ &- 2^{r+2}\Gamma(r+4) \\ &+ (3^{r+4} - 3 \cdot 2^{r+3})\Gamma(r+3) \\ &+ (3^r(162 - 81 \cdot 2^{r+2}) - 9 \cdot 2^{r+2})\Gamma(r+2) \end{aligned} \right\}$$

The first four moments of the CTAD Are given as

$$\begin{aligned}
 E(X) &= -\frac{50\lambda_2 + 81\lambda_1 - 347}{108\mu} \\
 E(X^2) &= -\frac{910\lambda_2 + 1215\lambda_1 - 4069}{324\mu^2} \\
 E(X^3) &= -\frac{5110\lambda_2 + 6075\lambda_1 - 18961}{324\mu^3} \\
 E(X^4) &= -\frac{23030\lambda_2 + 25515\lambda_1 - 77705}{243\mu^4}
 \end{aligned}$$

Variance of the CTAD is given as

$$Var(X) = \left[-\frac{910\lambda_2 + 1215\lambda_1 - 4069}{324\mu^2} \right] - \left[-\frac{50\lambda_2 + 81\lambda_1 - 347}{108\mu} \right]^2$$

The following table summarizes the statistical measures for various parameter values of μ , λ_1 , and λ_2 . It provides detailed insights into how these parameters affect the mean, variance, standard deviation, coefficient of variation, skewness, and kurtosis of the distribution.

Table 1. Statistical Measures for Varying Parameters.

μ	λ_1	λ_2	Mean (E[X])	(Var[X])	Std. Dev[X]	(CV[X])	(Skew[X])	(Kurt[X])
1.0	1.0	0.3	2.324	2.565	1.601	0.689	1.121	4.749
1.0	1.0	0.5	2.231481	2.424811	1.557181	0.697824	1.202731	5.035843
1.0	1.5	0.3	1.949074	2.292160	1.513988	0.776773	1.399889	5.574675
1.0	1.5	0.5	1.856481	2.082797	1.443190	0.777379	1.501185	6.092448
1.5	1.0	0.3	1.549383	1.139880	1.067651	0.689082	1.121207	4.749057
1.5	1.0	0.5	1.487654	1.077694	1.038120	0.697824	1.202731	5.035843
1.5	1.5	0.3	1.299383	1.018738	1.009325	0.776773	1.399889	5.574675
1.5	1.5	0.5	1.237654	0.925688	0.962127	0.777379	1.501185	6.092448

We have investigated the effects of the parameters μ , λ_1 , and λ_2 on the distribution characteristics of the CTAD model. The analysis reveals distinct patterns for each parameter across several statistical measures.

2.5. Moment Generating Function of the CTAD

The moment generating function (MGF) of a random variable X provides a way to uniquely determine the distribution of X if it exists in a neighbourhood of zero. The MGF of a random variable X is defined as $M_X(t) = E(e^{tX})$. Thus, then MGF of the CTAD is

$$\begin{aligned} E[e^{tX}] &= \int_0^\infty e^{tX} g(x) dx \\ &= \int_0^\infty e^{tX} \left[\mu^2 x e^{-\mu x} [\lambda_1 + 2(\lambda_2 - \lambda_1) (1 - (1 + \mu x)e^{-\mu x}) + 3(1 - \lambda_2) (1 - (1 + \mu x)e^{-\mu x})^2] \right] dx \end{aligned}$$

Integrating term by term reduces to

$$E(e^{tX}) = -\frac{\mu^2}{(\mu - t)^2 (2\mu - t)^3 (3\mu - t)^4} \left\{ \begin{aligned} &2t\mu^2 (150\mu^4 - 270t\mu^3 + 165t^2\mu^2 - 40t^3\mu + 3t^4) \lambda_2 \\ &+ t(3\mu - t)^4 (6\mu^2 - 6t\mu + t^2) \lambda_1 \\ &- 648\mu^7 + 1050t\mu^6 - 540t^2\mu^5 + 90t^3\mu^4 \end{aligned} \right\}$$

2.6. Entropy Measure

Entropy measures play critical roles in understanding and quantifying uncertainty, information content, and the properties of probability distributions in different scientific and engineering disciplines. In this section, we consider the Renyi entropy and the Shannon entropy.

2.6.1. Shannon entropy

Let X be a continuous random variable with pdf, $g(x)$. Then the Shannon entropy of X , written $H(X)$ is defined as

$$H(X) = - \int_{-\infty}^{\infty} g(x) \log[g(x)] dx$$

That is, the Shannon entropy for the CTAD is given as

$$\begin{aligned} H(X) &= - \int_{-\infty}^{\infty} \mu^2 x e^{-\mu x} [\lambda_1 + 2(\lambda_2 - \lambda_1) [1 - (1 + \mu x)e^{-\mu x}] + 3(1 - \lambda_2) [1 - (1 + \mu x)e^{-\mu x}]^2] \\ &\quad \times \log \left[\int_{-\infty}^{\infty} \mu^2 x e^{-\mu x} [\lambda_1 + 2(\lambda_2 - \lambda_1) [1 - (1 + \mu x)e^{-\mu x}] + 3(1 - \lambda_2) [1 - (1 + \mu x)e^{-\mu x}]^2] \right] dx \end{aligned}$$

2.6.2. Renyi entropy

Renyi entropy of order δ for a continuous probability distribution is defined as:

$$H_\alpha(X) = \frac{1}{1 - \delta} \log \int_0^\infty g(x)^\delta dx$$

Thus, the Renyi entropy for CTAD is

$$H_\alpha(X) = \frac{1}{1 - \delta} \log \left(\int_0^\infty (\mu^2 x e^{-\mu x} [\lambda_1 + 2(\lambda_2 - \lambda_1) (1 - (1 + \mu x)e^{-\mu x}) + 3(1 - \lambda_2) (1 - (1 + \mu x)e^{-\mu x})^2])^\delta dx \right)$$

2.6.3. Tsallis Entropy

Tsallis entropy of order q for a continuous probability distribution is defined as:

$$H_q(X) = \frac{1}{1 - q} \left(1 - \int_0^\infty g(x)^q dx \right)$$

Thus, the Tsallis entropy for the CTAD is given as

$$H_q(X) = \frac{1}{1-q} \left(1 - \int_0^\infty (\mu^2 x e^{-\mu x} [\lambda_1 + 2(\lambda_2 - \lambda_1) (1 - (1 + \mu x)e^{-\mu x}) + 3(1 - \lambda_2) (1 - (1 + \mu x)e^{-\mu x})^2])^q dx \right)$$

2.7. Order Statistics

Order statistics deal with the properties and behaviour of an ordered values from a sample of random variables. If we have a random sample of size n from CTAD, sorting these values in ascending order gives the order statistics. They are denoted as $X_{(1)}, X_{(2)}, \dots, X_{(n)}$, where:

1. $X_{(1)}$ is the smallest value (the first order statistic or the minimum),
2. $X_{(n)}$ is the largest value (the n th order statistic or the maximum).

Then the pdf of the k th order statistic, $X_{(k)}$ is given by

$$f_{k:n}(x) = \frac{n!}{(k-1)!(n-k)!} [G(x)]^{(k-1)} [1 - G(x)]^{(n-k)} \times g(x)$$

Substituting $G(x)$ and $g(x)$, we have

$$\begin{aligned} f_{k:n}(x) = & \frac{n!}{(k-1)!(n-k)!} \times \left[\lambda_1 [1 - (1 + \mu x)e^{-\mu x}] + (\lambda_2 - \lambda_1) [1 - (1 + \mu x)e^{-\mu x}]^2 \right. \\ & \left. + (1 - \lambda_2) [1 - (1 + \mu x)e^{-\mu x}]^3 \right]^{(k-1)} \left[1 - \lambda_1 [1 - (1 + \mu x)e^{-\mu x}] \right. \\ & \left. + (\lambda_2 - \lambda_1) [1 - (1 + \mu x)e^{-\mu x}]^2 + (1 - \lambda_2) [1 - (1 + \mu x)e^{-\mu x}]^3 \right]^{(n-k)} \\ & \times \mu^2 x e^{-\mu x} \left[\lambda_1 + 2(\lambda_2 - \lambda_1) [1 - (1 + \mu x)e^{-\mu x}] + 3(1 - \lambda_2) [1 - (1 + \mu x)e^{-\mu x}]^2 \right] \end{aligned}$$

The pdf of smallest order statistic of the CTAD is obtained when $k = 1$. Thus, by putting $k = 1$, the distribution of the minimum order statistic for the CTAD distribution is given as

$$\begin{aligned} f_{1:n}(x) = & n \left[1 - \lambda_1 (1 - (1 + \mu x)e^{-\mu x}) + (\lambda_2 - \lambda_1) (1 - (1 + \mu x)e^{-\mu x})^2 + (1 - \lambda_2) (1 - (1 + \mu x)e^{-\mu x})^3 \right]^{(n-1)} \\ & \times \left[\mu^2 x e^{-\mu x} \left(\lambda_1 + 2(\lambda_2 - \lambda_1) (1 - (1 + \mu x)e^{-\mu x}) + 3(1 - \lambda_2) (1 - (1 + \mu x)e^{-\mu x})^2 \right) \right] \end{aligned}$$

Also, the pdf of largest order statistic of the CTAD distribution can be obtained when $k = n$. Thus, by putting $k = n$, the maximum order statistic distribution for the CTAD obtained as

$$\begin{aligned} f_{n:n}(x) = & n \times \left[\lambda_1 [1 - (1 + \mu x)e^{-\mu x}] + (\lambda_2 - \lambda_1) [1 - (1 + \mu x)e^{-\mu x}]^2 + (1 - \lambda_2) [1 - (1 + \mu x)e^{-\mu x}]^3 \right]^{(n-1)} \\ & \times \mu^2 x e^{-\mu x} \left[\lambda_1 + 2(\lambda_2 - \lambda_1) [1 - (1 + \mu x)e^{-\mu x}] + 3(1 - \lambda_2) [1 - (1 + \mu x)e^{-\mu x}]^2 \right] \end{aligned}$$

2.8. Quantile Function

Given the cdf in Equation (6), to find the quantile function $Q(p)$, we set the cdf $G(x)$ equal to a probability p where $p \in [0, 1]$. That is,

$$p = \lambda_1 [1 - (1 + \mu x)e^{-\mu x}] + (\lambda_2 - \lambda_1) [1 - (1 + \mu x)e^{-\mu x}]^2 + (1 - \lambda_2) [1 - (1 + \mu x)e^{-\mu x}]^3. \quad (7)$$

To simplify, let y be defined as:

$$y = 1 - (1 + \mu x)e^{-\mu x}. \quad (8)$$

Substituting this into the equation for p , we obtain:

$$p = \lambda_1 y + (\lambda_2 - \lambda_1) y^2 + (1 - \lambda_2) y^3. \quad (9)$$

The equation is a cubic polynomial in y :

$$(1 - \lambda_2)y^3 + (\lambda_2 - \lambda_1)y^2 + \lambda_1 y - p = 0. \quad (10)$$

Once y is determined, we substitute back into Equation (7).

Solving this transcendental equation for x involves isolating x :

$$(1 + \mu x)e^{-\mu x} = 1 - y. \quad (11)$$

This equation does not generally yield a closed-form solution for x , so numerical methods are typically used to solve for x given y and thus for p .

3. Maximum Likelihood Estimation

Given a sample X_1, X_2, \dots, X_n , the likelihood function $L(\mu, \lambda_1, \lambda_2)$ is the joint probability density of the sample:

$$L(\mu, \lambda_1, \lambda_2) = \prod_{i=1}^n g(X_i; \mu, \lambda_1, \lambda_2)$$

The log-likelihood function $\ell(\mu, \lambda_1, \lambda_2)$ is given by:

$$\ell(\mu, \lambda_1, \lambda_2) = \sum_{i=1}^n \log g(X_i; \mu, \lambda_1, \lambda_2)$$

We express $g(x)$ in a more convenient form for differentiation. That is, we define

$$h(x, \mu) = 1 - (1 + \mu x)e^{-\mu x}$$

So,

$$g(x) = \mu^2 x e^{-\mu x} [\lambda_1 + 2(\lambda_1 - \lambda_1)h(x, \mu) + 3(1 - \lambda_2)h(x, \mu)^2]$$

Substituting $g(x)$ into the log-likelihood function:

$$\ell(\mu, \lambda_1, \lambda_2) = \sum_{i=1}^n \log (\mu^2 X_i e^{-\mu X_i} [\lambda_1 + 2(\lambda_2 - \lambda_1)h(X_i, \mu) + 3(1 - \lambda_2)h(X_i, \mu)^2])$$

To find the MLE, we differentiate the log-likelihood function with respect to μ , λ_1 , and λ_2 and set the derivatives to zero. Differentiation with respect to μ :

$$\frac{\partial \ell}{\partial \mu} = \sum_{i=1}^n \frac{1}{g(X_i)} \frac{\partial g(X_i)}{\partial \mu}$$

Differentiation with respect to λ_1 :

$$\frac{\partial \ell}{\partial \lambda_1} = \sum_{i=1}^n \frac{1}{g(X_i)} \frac{\partial g(X_i)}{\partial \lambda_1}$$

Differentiation with respect to λ_2 :

$$\frac{\partial \ell}{\partial \lambda_2} = \sum_{i=1}^n \frac{1}{g(X_i)} \frac{\partial g(X_i)}{\partial \lambda_2}$$

Solving these equations simultaneously will provide the MLEs for μ , λ_1 , and λ_2 . Python software will be used to estimate the parameters μ , λ_1 , and λ_2 using the MLE method.

The following table provides a comprehensive summary of the MLE for the parameters $\mu = 1.0$, $\lambda_1 = 0.5$, and $\lambda_2 = 0.2$ obtained from a simulation process across various sample sizes. It includes estimated values, absolute bias, Mean Squared Error (MSE), and Standard Error (SE) for each parameter, allowing for a clear comparison of the estimation performance as the sample size increases.

Table 2. Parameter Estimates of the QTED by Simulation.

Sample size	Estimate	—Bias—	MSE	SE
100	$\mu = 1.0484$	0.0484	0.0023	0.1433
	$\lambda_1 = 0.4066$	0.0934	0.0087	0.1433
	$\lambda_2 = 0.1753$	0.0247	0.0006	0.1433
150	$\mu = 0.9868$	0.0132	0.0002	0.1362
	$\lambda_1 = 0.5414$	0.0414	0.0017	0.1362
	$\lambda_2 = 0.1247$	0.0753	0.0057	0.1362
200	$\mu = 0.9895$	0.0105	0.0001	0.1188
	$\lambda_1 = 0.6252$	0.1252	0.0157	0.1188
	$\lambda_2 = -0.3236$	0.5236	0.2742	0.1188
300	$\mu = 0.9953$	0.0047	0.0000	0.0893
	$\lambda_1 = 0.3932$	0.1068	0.0114	0.0893
	$\lambda_2 = 0.3407$	0.1407	0.0198	0.0893
400	$\mu = 1.0430$	0.0430	0.0019	0.0747
	$\lambda_1 = 0.4307$	0.0693	0.0048	0.0747
	$\lambda_2 = 0.0301$	0.1699	0.0289	0.0747
500	$\mu = 1.0116$	0.0116	0.0001	0.0713
	$\lambda_1 = 0.5577$	0.0577	0.0033	0.0713
	$\lambda_2 = 0.1569$	0.0431	0.0019	0.0713
600	$\mu = 0.9838$	0.0162	0.0003	0.0666
	$\lambda_1 = 0.4552$	0.0448	0.0020	0.0666
	$\lambda_2 = 0.2163$	0.0163	0.0003	0.0666
700	$\mu = 0.9524$	0.0476	0.0023	0.0620
	$\lambda_1 = 0.5034$	0.0034	0.0000	0.0620
	$\lambda_2 = 0.3310$	0.1310	0.0172	0.0620
800	$\mu = 0.9982$	0.0018	0.0000	0.0577
	$\lambda_1 = 0.6816$	0.1816	0.0330	0.0577
	$\lambda_2 = 0.1117$	0.0883	0.0078	0.0577

The overall accuracy and precision of the MLE improve as the sample size increases. This is evident from the consistent reduction in the absolute bias, MSE, and SE as more data becomes available. Larger samples provide more reliable estimates, with smaller errors and greater consistency across the parameters. While the MLE performs well overall, there is variability in the performance depending on the parameter being estimated. For μ , the estimates are highly accurate even with smaller samples, but λ_1 and λ_2 exhibit more sensitivity to sample size, with λ_2 being particularly challenging to estimate accurately in smaller samples.

4. Application of the CTAD

The application of the CTAD is discussed in this section. The CTAD is applied to a real dataset to estimate its parameters. Additionally, three datasets will be explored to test the goodness of fit for CTAD. We use the following metrics: (LL , $-2LL$, AIC , BIC , and $CAIC$).

4.1. Dataset I

The dataset discussed here has previously been used by Choulakian & Stephens [6]. The dataset is the exceedances of flood peaks (measured in m3/s) of the Wheaton River near Carcross in Yukon Territory, Canada. The data entail 72 exceedances from 1958-1984.

Table 3. Exceedances of Wheaton River flood data.

1.7	2.2	14.4	1.1	0.4	20.6	5.3	0.7	13.0	12.0	9.3	1.4	18.7	8.5	25.5
11.6	14.1	22.1	1.1	2.5	14.4	1.7	37.6	0.6	2.2	39.0	0.3	15.0	11.0	7.3
22.9	1.7	0.1	1.1	0.6	9.0	1.7	7.0	20.1	0.4	14.1	9.9	10.4	10.7	30.0
3.6	5.6	30.8	13.3	4.2	25.5	3.4	11.9	21.5	27.6	36.4	2.7	64.0	1.5	2.5
27.4	1.0	27.1	20.2	16.8	5.3	9.7	27.5	2.5	27.0	1.9	2.8			

The descriptive statistics of the data are shown in Table 5 below.

Table 4. Descriptive Statistics.

Min	1st Qu.	Median	Mean	3rd Qu.	Max	Var	St. Dev.	Skew.	Kurt.
0.1	2.125	9.5	12.17	20.125	64.0	151.22	12.87	1.44	2.73

From the table, we can observe that the data has significant variability with some extreme values on the higher end, resulting in a right-skewed distribution. The central tendency measures (mean and median) are relatively close but highlight the influence of higher values on the mean. The high kurtosis indicates a distribution prone to producing outliers.

The goodness of fit of the CTAD distribution is compared with the probability distributions from the Ailamujia family of distribution. That is, the pdf in Equation 1 and the quadratic transmuted Ailamujia distribution (QTAD) given by Adetunji [1] and is defined as

$$f(x) = \theta^2 x e^{-\theta x} [1 - \lambda + 2x e^{-\theta x} + 2\lambda \theta x e^{-\theta x}] \quad x \in \mathbb{R}, \theta > 0 \quad |\lambda| \leq 1$$

Table 5 presents the parameters estimates for the CTAD, QTAD and Ailamujia distribution obtained through MLE.

Table 5. Parameter Estimates via MLE.

Distribution	Parameter	MLE Estimate	Standard Error
CTAD distribution	$\mu, \lambda_1, \lambda_2$	0.1988, 1.0000, -0.6106	0.0266, 1.2232, 1.5991
QTAD	μ, α	0.1495, 0.3093	0.0106 1.0530
Ailamujia distribution	μ	0.1639	0.0137

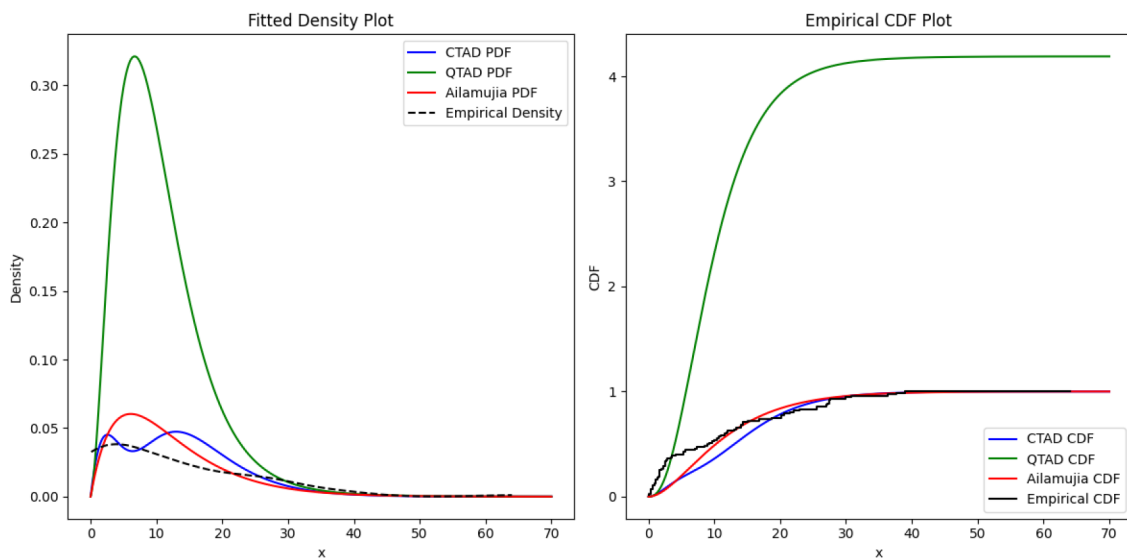
Table 6 presents the goodness-of-fit metrics to evaluate how well the distributions fit the given dataset. The distribution that minimizes the values of the aforementioned goodness-of-fit metrics would provide the best fit for the given dataset.

Table 6. Model Comparison Criteria.

Distribution	LL	-2LL	AIC	BIC	CAIC
CTAD distribution	-268.72	537.43	543.43	550.26	543.79
QTAD	-273.74	547.47	551.47	554.02	551.64
Ailamujia distribution	-274.98	549.96	551.96	554.24	552.02

It can be seen that the CTAD distribution consistently yields the smallest values and therefore provides the best fit for the data.

We present fitted density plots that compare the empirical distribution of the data with various theoretical distributions, specifically the CTAD, QTAD, and Ailamujia distributions.

**Figure 5.** Fitted density and empirical cdf plots.

The plot allows for a direct comparison between the empirical density and the fitted distributions. It is crucial to assess which model best represents the data, especially in terms of capturing the tail behavior and the peak density. The CTAD distribution appears to fit the data exceptionally well near the peak, indicating that it is the most suitable model

among the three for this dataset.

4.2. Dataset II

The dataset considered here comprises cumulative COVID-19 death counts for Ghana, spanning from March 21, 2020, to May 21, 2020, as obtained from Our World in Data [12].

Table 7. Cumulative COVID-19 death counts for Ghana.

1	1	2	2	4	4	4	5	5	5	5	5
5	5	5	5	5	5	6	6	6	8	8	8
8	8	8	8	8	8	9	9	9	9	9	10
10	11	11	16	16	17	17	18	18	18	18	18
18	18	22	22	22	22	24	24	28	29	29	29
31	31	31									

The following table summarizes the descriptive statistics of the cumulative COVID-19 death counts for Ghana, providing insights into the distribution and central tendencies of the data.

Table 8. Descriptive Statistics.

Min	1st Qu.	Median	Mean	3rd Qu.	Max	Var	St. Dev.	Skew.	Kurt.
1	5	9	12.56	18	31	76.48	8.75	0.75	-0.62

The Descriptive Statistics summarizes the cumulative COVID-19 death counts for Ghana. The dataset's minimum value is 1, reflecting the early stage of the pandemic. The variance of 76.48 and standard deviation of 8.75 suggest significant variability in the death counts over time. The skewness of 0.75 points to a distribution slightly skewed to the right, with higher values being more common towards the

latter part of the dataset. The kurtosis of -0.62 indicates that the distribution has lighter tails compared to a normal distribution, suggesting fewer extreme cumulative death counts.

The goodness of fit for the CTAD is evaluated in comparison with the following distributions:

1. Cubic Transmuted Gumbel (CTGD), Celik (2018)

$$f(x) = \frac{1}{\sigma} \exp \left(- \left[\frac{x - \mu}{\sigma} + \exp \left(- \frac{x - \mu}{\sigma} \right) \right] \right) \times \left[\lambda_1 + 2(\lambda_2 - \lambda_1) \exp \left(- \exp \left(- \frac{x - \mu}{\sigma} \right) \right) + 3(1 - \lambda_2) \left(\exp \left(- \exp \left(- \frac{x - \mu}{\sigma} \right) \right) \right)^2 \right]$$

where $\lambda_1 \in [0, 1]$, $\lambda_2 \in [-1, 1]$, $\mu > 0$, $\sigma > 0$

2. Cubic Transmuted Fr chet (CTFD), Celik (2018)

$$f(x) = \frac{\alpha}{\sigma} \left(\frac{x}{\sigma} \right)^{-1-\alpha} \exp \left[- \left(\frac{x}{\sigma} \right)^{-\sigma} \right] \times \left[\lambda_1 + 2(\lambda_2 - \lambda_1) \exp \left(- \left(\frac{x}{\sigma} \right)^{-\sigma} \right) + 3(1 - \lambda_2) \left(\exp \left(- \left(\frac{x}{\sigma} \right)^{-\sigma} \right) \right)^2 \right]$$

for $\lambda_1 \in [0, 1]$, $\lambda_2 \in [-1, 1]$, $\alpha > 0$, $\sigma > 0$

3. Cubic Transmuted Weibull (CTWD), Granzotto et al. (2017)

$$f(x) = \frac{\mu}{\beta} x^{\mu-1} \exp \left(- \left(\frac{x}{\beta} \right)^{\mu} \right) \times \left[(3 - \lambda_1 - \lambda_2) + 2(\lambda_1 + 2\lambda_2 - 3) \exp \left(- \left(\frac{x}{\beta} \right)^{\mu} \right) + 3(1 - \lambda_2) \exp \left(- 2 \left(\frac{x}{\beta} \right)^{\mu} \right) \right]$$

for $x > 0$, $\mu > 0$, $\beta > 0$, $\lambda_1 \in [0, 1]$, $\lambda_2 \in [-1, 1]$

Table 9 presents the parameter estimates for the CTAD, CTGD, CTFD, and CTWD obtained through MLE.

Table 9. Parameter Estimates via MLE.

Distribution	Parameter	MLE Estimate	Standard Error
CTAD	$\mu, \lambda_1, \lambda_2$	0.1676, 1.000, 0.7188	0.2651, 8.6401, 8.4645
CTGD	$\mu, \sigma, \lambda_1, \lambda_2$	0.4808, 6.5685, 0.0000, -0.7589	1.8355, 1.2396, 0.9360, 0.9321
CTFD	$\alpha, \sigma, \lambda_1, \lambda_2$	0.7043, 2.0691, 0.2715, -0.2724	0.5779, 0.8317, 0.8666, 1.0558
CTWD	$\mu, \beta, \lambda_1, \lambda_2$	0.7607, 4.5578, 0.0000, -0.3960	0.5120, 4.1475, 0.7373, 0.8329

Table 10 presents the goodness-of-fit metrics to evaluate how well the distributions fit the given dataset.

Table 10. Model Comparison Criteria.

Distribution	LL	-2LL	AIC	BIC	CAIC
CTAD	-212.01	424.01	430.01	436.39	439.39
CTGD	-213.67	427.34	435.34	443.85	447.85
CTFD	-192.75	385.49	393.49	402.00	406.00
CTWD	-235.53	471.06	479.06	487.58	491.57

These metrics provide a comparative overview, indicating that the CTFD distribution fits the dataset better than the others, while the CTAD offers a competitive fit among the compared models.

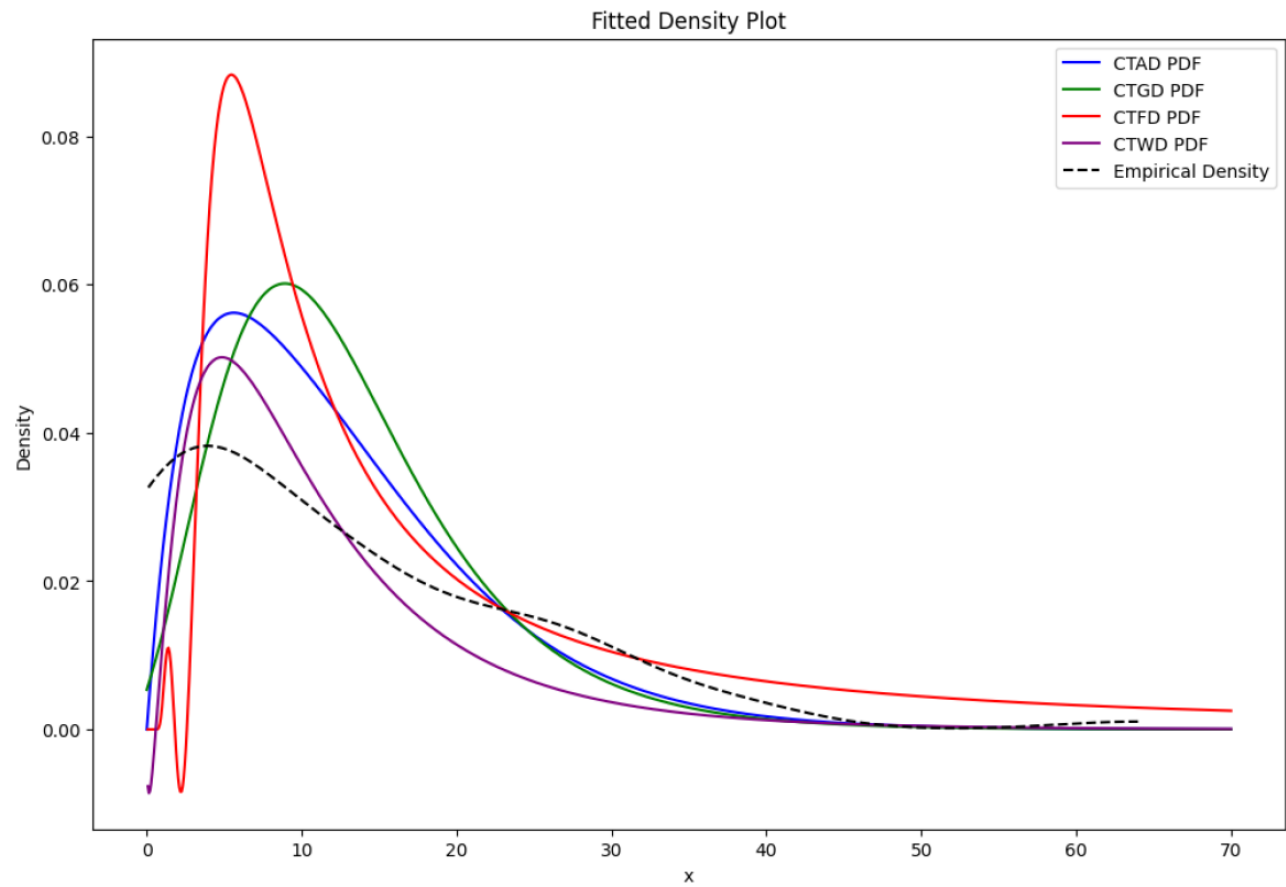


Figure 6. fitted density plot.

4.3. Dataset III

The dataset discussed here contains daily confirmed COVID-19 cases for Ghana over a 90-day period, ranging from March 14, 2020, to June 11, 2020. The data, obtained from Our World in Data, represent the actual number of reported cases on each day within this time frame.

Table 11. Daily confirmed COVID-19 cases spanning over 90 days for Ghana.

3	3	0	1	0	4	5	3	4	4
26	40	39	5	4	11	0	9	34	9
1	0	9	0	73	26	65	0	30	158
0	70	0	5	0	193	208	0	0	112
0	125	0	271	0	121	0	403	0	95
0	550	0	372	0	921	251	0	437	427
281	122	108	97	0	0	361	173	0	217
131	66	125	309	186	0	313	152	302	0
227	251	337	283	294	176	272	291	0	157

The following descriptive statistics summarize the daily confirmed COVID-19 cases in Ghana over a 90-day period:

Table 12. Descriptive Statistics.

Min	1st Qu.	Median	Mean	3rd Qu.	Max	Var	St. Dev.	Skew.	Kurt.
1	22.250	123.5000	161.843	271.250	921	27724.85	166.508	1.742	4.488

The dataset of daily confirmed COVID-19 cases in Ghana over 90 days shows an average (mean) of 161.84 cases, with a median of 123.5. The data exhibits significant variability, with a standard deviation of 166.51 and a variance of 27,724.85, highlighting substantial fluctuations in daily cases. The positive skewness of 1.74 suggests a long right tail, meaning a few days had very high case counts, and the kurtosis of 4.89 indicates that these high values were more extreme than in a

normal distribution.

The goodness of fit for the CTAD is compared against several well-known distributions, including the Skew Normal Distribution (SKD), Generalized Normal Distribution (GND), Exponentiated Weibull Distribution (EWD), Generalized Gamma Distribution (GGD), and Nakagami Distribution (ND).

1. SND

$$f(x) = \frac{2}{\omega} \phi\left(\frac{x-\xi}{\omega}\right) \Phi\left(\alpha \frac{x-\xi}{\omega}\right)$$

where $\phi(\cdot)$ is the standard normal pdf, $\Phi(\cdot)$ is the standard normal cdf, and $\xi \in \mathbb{R}, \omega > 0, \alpha \in \mathbb{R}$

2. GND

$$f(x) = \frac{\beta}{2\alpha\Gamma(1/\beta)} \exp\left(-\left(\frac{|x-\mu|}{\alpha}\right)^\beta\right)$$

where $\mu \in \mathbb{R}, \alpha > 0, \beta > 0$

3. EWD

$$f(x) = \alpha\beta\lambda^{-\beta}x^{\beta-1} \exp\left(-\left(\frac{x}{\lambda}\right)^\beta\right) \left(1 - \exp\left(-\left(\frac{x}{\lambda}\right)^\beta\right)\right)^{\alpha-1}$$

where $\alpha > 0, \beta > 0, \lambda > 0$

4. GGD

$$f(x) = \frac{\gamma}{\beta^\alpha\Gamma(\alpha/\gamma)} x^{\alpha-1} \exp\left(-\left(\frac{x}{\beta}\right)^\gamma\right)$$

where $\alpha > 0, \beta > 0, \gamma > 0$

5. ND

$$f(x) = \frac{2m^m}{\Gamma(m)\Omega^m} (x-\mu)^{2m-1} \exp\left(-\frac{m}{\Omega}(x-\mu)^2\right)$$

where $m \geq \frac{1}{2}, \Omega > 0, \mu \in \mathbb{R}$

Table 13. Parameter Estimates via MLE.

Distribution	Parameter	MLE Estimate	Standard Error
CTAD	$\mu, \lambda_1, \lambda_2$	0.0157, 1.000, -0.8285	0.0027, 1.0000, 1.6371
SKD	ϕ, Ω, α	161.8438, 166.5078, 0.0000	1.000, 1.0000, 1.0000
GND	μ, σ, β	136.0361, 173.7547, 1.3532	33.6978, 45.0197, 0.4544
EWD	α, β, γ	0.8857, 0.0100, 0.7714	18.4557, 1.5004, 21.2150
GGD	α, β, γ	0.0273, 16.1587, 0.0183	106.1167, 225.0508, 37.7200
ND	m, Ω, μ	0.0100, 24.5434, 0.6629	1.000, 219.6294, 6.8165

Table 14. Model Comparison Criteria.

Distribution	LL	-2LL	AIC	BIC	CAIC
CTAD	-417.12	834.23	840.23	846.71	847.71
SKD	-418.17	836.25	842.35	848.83	849.83
GND	-416.18	832.35	838.35	844.83	845.83
EWD	-385.45	770.90	776.90	783.38	783.37
GGD	-323.97	647.95	653.95	660.43	661.43
ND	-570.32	1140.65	1146.65	1153.12	1154.12

While the CTAD performs reasonably well, especially considering it is a newly developed distribution, it does not outperform the Generalized Gamma Distribution and Exponentiated Weibull Distribution in most criteria. This indicates that, although CTAD is competitive, the other distributions offer slightly better fit or more efficient use of parameters given the data set.

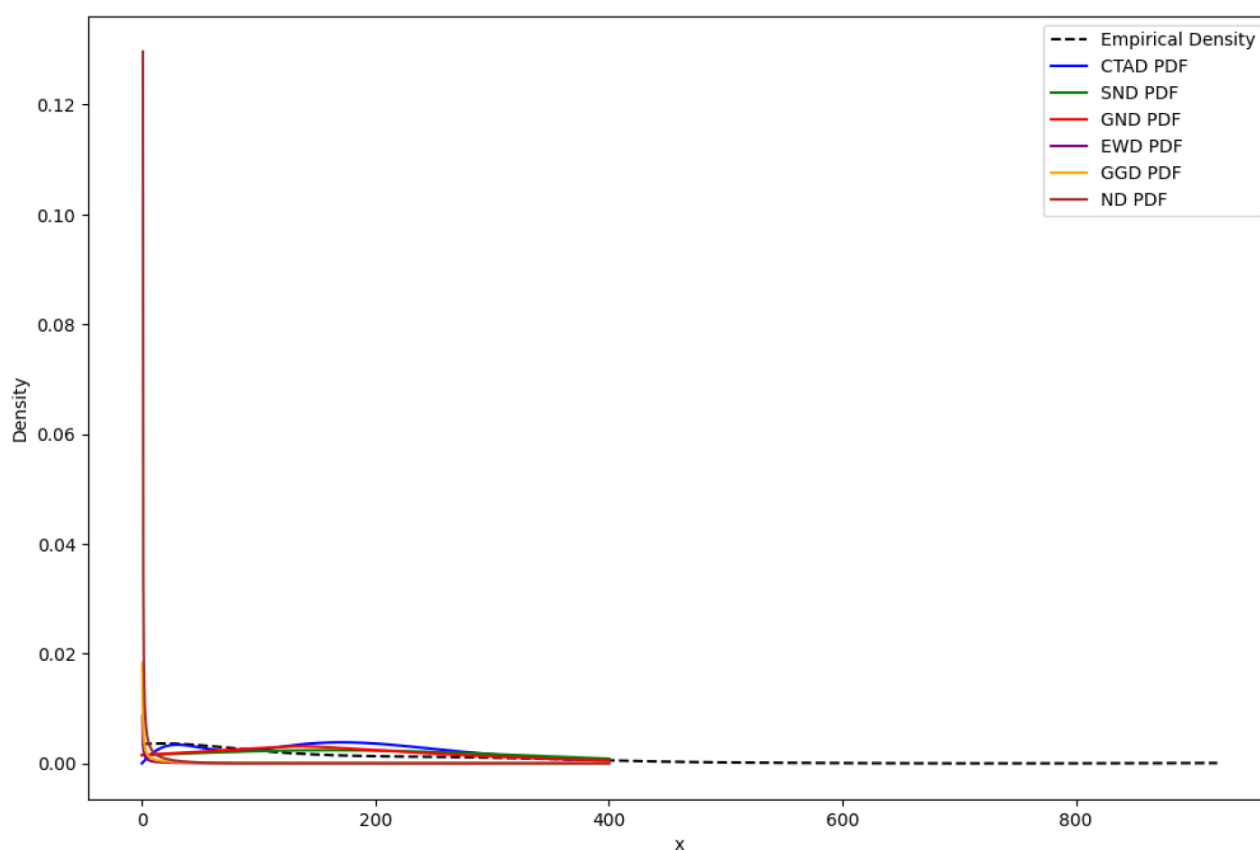


Figure 7. Fitted density plot.

5. Conclusion

In this study, we evaluated the goodness-of-fit of the CTAD, developed as an extension of CRT-type I, against several well-established distributions using three distinct datasets. For Dataset I, which contains exceedances of flood peaks from the Wheaton River, the CTAD showed competitive performance, surpassing the QTAD and Ailamujia distributions based on key model comparison criteria such as AIC and BIC.

In Dataset II, comprising cumulative COVID-19 death counts for Ghana, the CTAD also performed favourably compared to the CTGD, CTFD, and CTWD distributions. Specifically, it demonstrated a better fit than the CTWD but was outperformed by the CTFD, as evidenced by lower AIC and BIC values. Dataset III, which details daily confirmed COVID-19 cases for Ghana, revealed that the CTAD had a robust fit compared to the SKD, GND, EWD, and GGD distributions, although it was less effective than the EWD and GGD in terms of AIC and BIC. Notably, the CTAD provided a better fit than the Nakagami distribution, which highlights its effectiveness in modelling COVID-19 case data.

Overall, the CTAD presents a valuable alternative to existing distributions, particularly in scenarios involving complex data patterns. Its performance across different datasets demonstrates its flexibility and effectiveness. However, the results also suggest that while the CTAD is competitive, certain alternative distributions may offer superior fit in specific contexts. Future work could further refine the CTAD and explore its applications in other domains to fully assess its potential.

Abbreviations

CTAD	Cubic Transmuted Ailamujia Distribution
QTAD	Quadratic Transmuted Ailamujia Distribution
CTGD	Cubic Transmuted Gumbel Distribution
CTFD	Cubic Transmuted Fréchet Distribution
CTWD	Cubic Transmuted Weibull Distribution
SND	Skew Normal Distribution
GND	Generalized Normal Distribution
EWD	Exponentiated Weibull Distribution
GGD	Generalized Gamma Distribution
ND	Nakagami Distribution

ORCID

0009-0008-5147-6128 (Jones Asante Manu)

0009-0002-9215-6143 (Samuel Darkwah)

Author Contributions

Jones Asante Manu: Conceptualization, Data curation, Formal Analysis, Funding acquisition, Investigation, Methodology, Project administration, Resources, Software,

Validation, Visualization, Writing - original draft, Writing - review & editing

Samuel Darkwah: Conceptualization, Data curation, Formal Analysis, Methodology, Resources, Software, Supervision, Visualization, Writing - original draft, Writing - review & editing

Funding

This research received no specific grant from any funding agency in the public, commercial, or not-for-profit sectors.

Conflicts of Interest

The authors declare no conflicts of interest.

References

- [1] Adetunji, A. A. (2023). Transmuted Ailamujia Distribution with Applications to Lifetime Observations. *American Journal of Pure and Applied Sciences*, 21(1), 1-11. <https://doi.org/10.9734/AJPAS/2023/v21i1452>
- [2] Aijaz, A., Ahmad, A., & Tripathi, R. (2020). Inverse analogue of Ailamujia distribution with statistical properties and applications. *Asian Research Journal of Mathematics*, 16(9), 36-46.
- [3] AL-Kadim, K. A., & Mohammed, M. H. (2017). The Cubic Transmuted Weibull Distribution. *Journal of Babylon University/Pure and Applied Sciences*, 25(3), 862-876.
- [4] Burr, I. W. (1942). Cumulative frequency functions. *Annals of Mathematical Statistics*, 13, 215-232. <https://doi.org/10.1214/aoms/1177731607>
- [5] Celik, N. (2018). Some Cubic Rank Transmuted Distributions. *Journal of Applied Mathematics, Statistics and Informatics*, 14(2), 27-43.
- [6] Choulakian, V., & Stephens, M. A. (2001). Goodness-of-fit tests for the generalized Pareto distribution. *Technometrics*, 43(4), 478-484.
- [7] Cordeiro, G. M., & Castro, M. de. (2011). A new family of generalized distributions. *Journal of Statistical Computation and Simulation*, 81, 883-898.
- [8] Eugene, N., Lee, C., & Famoye, F. (2002). Beta-normal distribution and its applications. *Communications in Statistics-Theory and Methods*, 31, 497-512.
- [9] Granzotto, D. C. T., Louzada, F., & Balakrishnan, N. (2017). Cubic Rank Transmuted Distributions: Inferential Issues and Applications. *Journal of Statistical Computation and Simulation*, 87(14), 2760-2778.

- [10] Marshall, A. W., & Olkin, I. (1997). A new method for adding a parameter to a family of distributions with application to the exponential and Weibull families. *Biometrika*, 84, 641-652. <https://doi.org/10.1093/biomet/84.3.641>
- [11] Lv, H. Q., Gao, L. H., & Chen, C. L. (2002). Ailamujia distribution and its application in supportability data analysis. *Journal of Academy of Armored Force Engineering*, 16(3), 48-52.
- [12] Our World in Data. (2024). Coronavirus pandemic (COVID-19). <https://ourworldindata.org/coronavirus>
- [13] Pan, G. T., Wang, C. L., Huang, Y. B., & Dang, M. T. (2009). The research of interval estimation and hypothetical test of small sample of Ailamujia distribution. *Application of Statistics and Management*, 28(3), 468-472.
- [14] Pearson, K. (1895). Contributions to the mathematical theory of evolution, II: Skew variation in homogeneous material. *Philosophical Transactions of the Royal Society*, 186, 343-414. <https://doi.org/10.1098/rsta.1895.0010>
- [15] Rather, A., Subramanian, C., Shafi, S., Malik, K. A., Ahmad, P. J., Para, B. A., & Jan, T. A. (2018). New size biased distribution with Applications in Engineering and Medical Science. *IJSRMSS*, 5(4), 75-85.
- [16] Rahman, M. M., AL-Zahrani, B., & Shahbaz, M. Q. (2018). A General Transmuted Family of Distributions. *Pakistan Journal of Statistics and Operation Research*, 14(2), 451-469.
- [17] Uzma, J., Kawsar, F., & Ahmad, S. P. (2017). On weighted Ailamujia distribution and its applications to life time data. *Journal of Statistics Applications and Probability an International Journal*, 6(3), 619-633.